energies

MDPI

Article

Channel Access in Wireless Smart Grid Networks Operating under ETSI Frame-Based Equipment Rules

Marcin Karcz and Szymon Szott *

Institute of Telecommunications, Faculty of Computer Science, Electronics and Telecommunications, AGH University of Krakow, 30-059 Kraków, Poland; karczm@student.agh.edu.pl
* Correspondence: szymon.szott@agh.edu.pl

Abstract: Smart grid operators seeking to extend their wireless network capacity can use unlicensed bands. However, devices in these shared bands must follow rules such as Listen Before Talk (LBT), standardized by ETSI. In this paper, we focus on the performance of the frame-based equipment (FBE) version of LBT channel access. We design, implement, and validate a fully functional FBE channel access simulator. Next, we conduct an extensive performance analysis of the FBE variants encountered in the literature, focusing on channel efficiency and fairness in upper-bound and coexistence scenarios. Our study leads to several conclusions about the operation of FBE-based devices, including the need for proper configuration of channel access parameters to ensure fairness and optimal performance. We also observe generally poor coexistence among FBE variants: the highest Jain's fairness index was only 0.88, with an average normalized channel efficiency of 0.76. Therefore, we identify several open research areas in the field, such as the need for further development of parameter adaptation algorithms, the deployment of an external controller to update channel access parameters, and new FBE designs with better coexistence qualities.

Keywords: channel access; wireless networks; Listen Before Talk; unlicensed bands

Citation: Karcz, M.; Szott, S. Channel Access in Wireless Smart Grid Networks Operating under ETSI Frame-Based Equipment Rules. *Energies* **2024**, *17*, 153. https://doi.org/10.3390/en17010153

Academic Editor: Ahmed Abu-Siada

Received: 1 December 2023
Revised: 22 December 2023
Accepted: 25 December 2023
Published: 27 December 2023

1. Introduction

Smart grid operators are seeking to extend their wireless network capacity to accommodate the traffic requirements of modern industrial networks [1,2]. This capacity can be extended through licensed bands (with cognitive radio) [3] or in unlicensed (shared) bands [4]. The latter is usually more cost-effective and the recently released 6 GHz band provides new spectrum resources [5]. However, operation in unlicensed bands requires appropriate channel sharing methods. The European Telecommunications Standards Institute (ETSI) specification [6] defines such rules, collected under the umbrella term Listen Before Talk (LBT). Two separate LBT variants are defined in the specification, for load-based equipment (LBE) and frame-based equipment (FBE). The former implements the random-based channel access mechanism of the IEEE 802.11 standard. The latter, however, follows a scheduled-access approach and is designed for industrial and smart grid networks, where nodes transmit in duty cycles [7].

A good candidate for implementing FBE channel access in shared bands is found in the fifth generation of wireless cellular networks in new radio unlicensed (NR-U). For coexistence with other radio technologies, NR-U already implements LBT as the channel access protocol [5] and NR-U studies usually assume the LBE variant [8–15]. However, as a cellular radio access technology, NR-U inherits a scheduled access approach in which nodes have to start transmissions at predefined slot boundaries. This requirement is not a good fit for the random access nature of LBE, because the end of an LBE channel access procedure does not have to match the closest slot boundary. Additional measures are required to guarantee an exact match of the start of a transmission and the synchronization slot boundary, e.g., transmitting a reservation signal [16]. Conversely, the fixed frame structure

of FBE seems to be an exact, out of the box solution for synchronizing NR-U transmissions with slot boundaries, which can potentially bring better utilization of channel resources [17]. Therefore, the significance of researching FBE can be summarized as follows: it has support from the industry (since it has been included as part of an ETSI specification); its design is tailored to the periodic traffic requirements of industrial networks; it follows simpler design principles than LBE, making it easier for implementation; and its design conforms with the requirements of cellular networks operating in unlicensed bands. However, the main challenge of implementing FBE is that it lacks a contention resolution mechanism [17], which can lead to unwanted behavior when multiple FBE nodes contend for the channel.

In this paper, we focus on industrial network settings, i.e., controlled, greenfield environments, in which FBE devices can be assured exclusive channel access but must nevertheless compete among themselves [18]. Therefore, the case where multiple FBE nodes contend for the channel is an interesting aspect to study. Furthermore, some FBE variants have not yet been evaluated in terms of performance. Therefore, our goal is to evaluate the performance of FBE-based channel access mechanisms. In this paper, we bring the following contributions:

- a performance evaluation of individual FBE variants in homogeneous networks, i.e., with all nodes operating under a single variant, to determine their contention resolution capabilities;
- a performance evaluation of FBE variants in heterogeneous networks, i.e., with all nodes using one of two competing FBE variants, to determine their coexistence capabilities;
- a set of conclusions regarding FBE configuration, performance, and coexistence as well as the identification of open research areas in this field;
- an FBE channel access simulator, released as open source for the research community, that is well suited for discovering issues of low or unfair channel access probabilities;
- an overview and classification of FBE variants proposed in the literature, including two of our own proposals.

The remainder of the paper is organized as follows. First, we give an overview of the state of the art in Section 2. Then, in Section 3, we provide a succinct description of the operation of FBE and its variants found in the literature. Next, we describe and validate our simulation tool for studying FBE performance in Section 4. We present the results of our thorough performance analysis of the FBE variants in Section 5. Finally, we summarize the paper and outline future work in Section 6. We hope that this work will facilitate further study and performance improvement of FBE-based solutions.

2. Literature Review

FBE channel access has received less interest from researchers than LBE. Most existing papers evaluate FBE performance in long term evolution (LTE) license-assisted access (LAA) networks, the predecessor of NR-U, and typically in LTE LAA and Wi-Fi coexistence scenarios [19–23]. Both Sutton et al. [24] and Abdelfattah et al. [25] evaluate the limits of FBE with Markov chains and conclude that the strict duty cycle scheme of FBE causes domination by the competing (Wi-Fi) devices. Park et al. [26] provide an analytical model of FBE to determine latency. Maldonado et al. [27] consider a fully coordinated FBE and LBE approach, where each FBE node calculates its uplink/downlink ratio during idle periods and communicates this to a central controller, which calculates an appropriate frame structure for the connected FBE nodes. Le et al. [28] propose dynamic switching between LBE and FBE in which the transmitting nodes switch the channel access mechanisms based on frame priority. Furthermore, Nobar et al. [29] design an algorithm for the joint channel assignment problem and transmission duration optimization for FBE in Wi-Fi coexistence scenarios while Bajracharya et al. [17] design a machine-learning-based adaptive duty cycling mechanism for NR-U coexisting with other radio technologies. The challenges and opportunities of the available channel access mechanisms are summarized in [5]. In terms of stand-alone FBE analysis, Wei et al. [30] and Li et al. [31] optimize FBE channel access

considering power consumption. Furthermore, there have been proposals of FBE variants, e.g., discussed in 3GPP meetings [32–34] and in the literature [35,36].

We distinguish ourselves from previous work by assessing the channel access performance of FBE in terms of channel utilization and fairness among contending devices, both for the standardized version of FBE and its variants. Furthermore, we provide a coexistence study between FBE variants that is also lacking in the literature.

3. Channel Access

In this section, we describe the channel access procedures for FBE, first as standardized by ETSI and then several modifications proposed in the literature.

3.1. Frame-Based Equipment

The FBE channel access rules are part of the LBT scheme defined in ETSI EN 301 893 [6]. In LBT, the nodes perform a clear channel assessment (CCA) immediately before each transmission. The CCA is performed during a single observation slot, which lasts at least 9 µs. For FBE nodes, the start of a transmission signifies the beginning of the duty cycle, called a fixed frame period (FFP). FFP can last from 1 to 10 ms and a node can manipulate its duration, but changes cannot occur more often than once every 200 ms. Each channel access duration is limited by the channel occupancy time (COT), which in turn cannot exceed 95% of the FFP. During a single COT, a node can perform multiple transmissions without repeating the CCA only if the gap between consecutive transmissions is not greater than 16 µs. Otherwise, an additional CCA is required to determine the status of the channel. A receiver can skip CCA and immediately respond with an acknowledgment after successful data reception, but only if the acknowledgment duration does not exceed the COT. The time between the end of the COT and the beginning of the next FFP is called the idle period and must be at least 5% of the COT, with a minimum of 100 µs. If a CCA operation is unsuccessful (i.e., indicative of a busy channel), an FBE node must refrain from transmission (referred to as muting) and perform a CCA before the next FFP. Figure 1 illustrates the operation of FBE and the various time periods. Henceforth, we refer to this mode of operation as standard FBE.

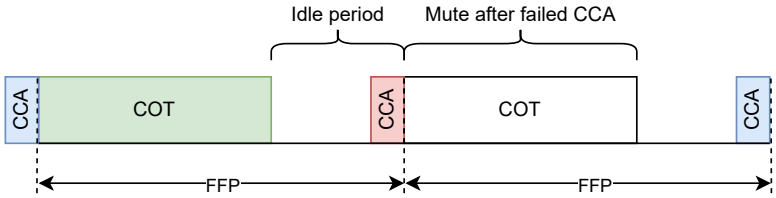

Figure 1. Example of standard FBE operation. A successful CCA precedes the first COT. The second CCA is unsuccessful, hence the node refrains from transmitting in the second FFP.

Standard FBE and most variants described below follow a periodic FFP scheme, so the synchronization of node COTs impacts performance. The case in which all nodes start their FFPs simultaneously is referred to in the literature as the synchronous mode. The benefits of this approach are related to the synchronization of base stations in cellular systems [10]. However, in unlicensed bands, this can lead to collisions (Figure 2a). An alternative is the asynchronous mode, in which nodes start their FFPs independently, which we model by stating that each node is delayed by a shift. We also introduce the concept of perfect node coordination—the state in which the shift of nodes is optimally configured so that they can transmit in consecutive FFPs without collisions. An example of perfect node coordination is shown in Figure 2b.

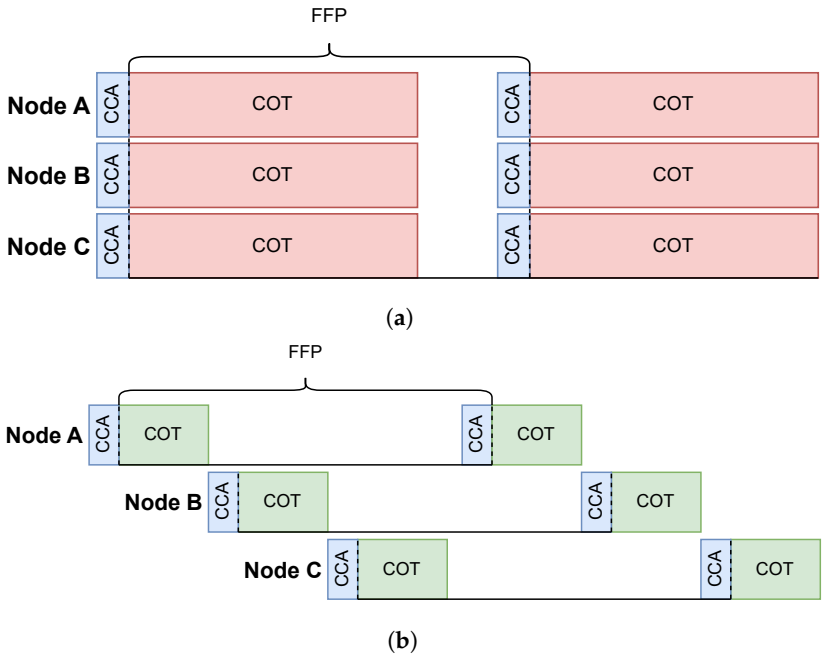

Figure 2. FBE node synchronization issues in an example three-node network: (**a**) synchronous mode leads to constant collisions, (**b**) perfect node coordination—the FFP of each node is delayed by evenly spaced shifts ensuring round-robin transmissions (if CCAs do not overlap with COTs).

3.2. FBE Variants

The basic FBE algorithm is trivial and does not offer any contention resolution mechanisms. From Figure 1 it is apparent that the only airtime available to other contending nodes to initiate their transmissions is during the idle period. Therefore, a single node can easily dominate channel access (as we show in Section 4). Several variants of FBE have been proposed (Figure 3) to overcome the lack of a contention resolution mechanism, and we describe their operation in the following.

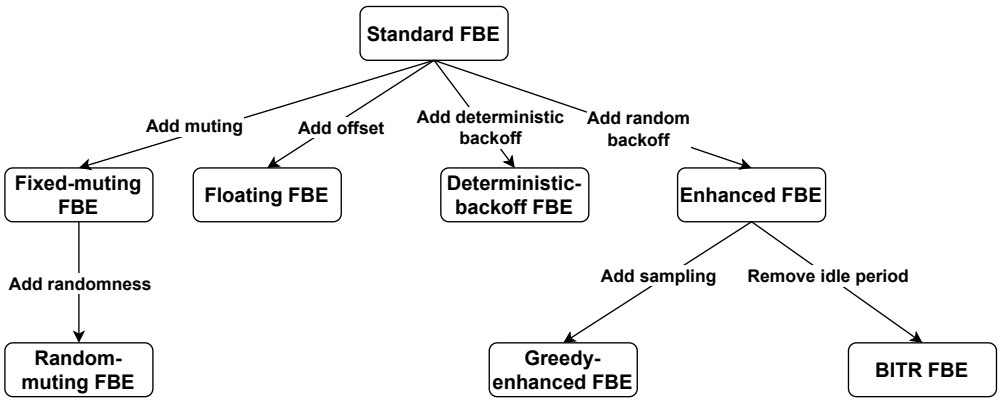

Figure 3. Classification of FBE variants proposed in the literature to enhance FBE with contention resolution capabilities.

3.2.1. Fixed-Muting FBE

We begin with fixed-muting FBE, our first proposal to improve FBE channel access. This proposal extends the basic functionality of FBE in that after a successful transmission, the transmitting node refrains from transmission for the subsequent N (muted) periods. This means that CCA procedures are also omitted, both at the end of the period with the successful transmission and during the muted periods.

3.2.2. Random-Muting FBE

A more advanced version of fixed-muting is random-muting FBE [32]. Before accessing the channel, a node selects a random number M from the range $[1, M_{max}]$, where M is the number of consecutive FFPs with successful transmissions. If the channel is accessed for M consecutive periods, then the node is muted for N random periods, selected from the range $[1, N_{max}]$. In other words, if the channel becomes blocked by M consecutive transmissions from a single node, that node will defer channel access for the next N periods.

3.2.3. Floating FBE

Floating FBE [33] changes the frame structure described in Section 3.1: instead of having the COT placed at the beginning and CCA at the end of the FFP, the COT is now directly preceded by CCA (Figure 4). Moreover, a node is allowed to start its CCA with a random offset within an FFP. This offset is selected as

$$offset = rand(0, slots) \times O_s \quad (1)$$

where $rand()$ — returns a random integer from a uniform distribution;
$slots$ = $\left\lfloor \frac{IP-CCA}{O_s} \right\rfloor$;
O_s — observation slot duration;
IP — idle period duration;
CCA — CCA duration.

A similar offset approach is presented in [37].

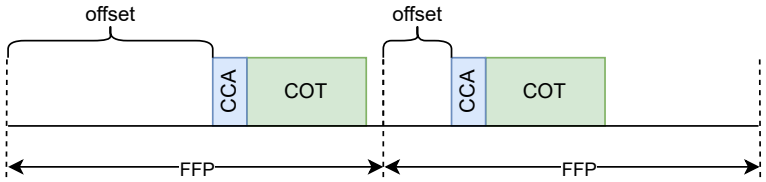

Figure 4. Operation of floating FBE.

3.2.4. Deterministic-Backoff FBE

Deterministic-backoff FBE (DB FBE) is our second proposed variant based on the deterministic-backoff algorithm [38]. Instead of muting for a number of FFPs after a data transmission, DB FBE nodes refrain from accessing the channel (i.e., backoff) for several FFPs before a transmission. This backoff procedure is governed by the variable b, which indicates the number of FFPs during which a node cannot access the channel. Initially, b is set to an initial backoff value α. During the backoff periods, the node monitors the channel and decrements b after each empty FFP. An FFP is determined to be empty on the basis of a single CCA, which is conducted at the beginning of the FFP. If the node detects a busy channel, then an interrupt counter i is incremented. Once b reaches zero, the node can start transmitting. If a collision occurs, the node increments a retransmission counter r, otherwise r is set to zero. After each transmission, a new backoff value is selected. If the value of r modulo r_{max} (maximum number of retransmissions) is less than a threshold of β, the node sets $b = \alpha + i$ and resets i, in the other case b is randomly selected from the range of $[1, r_{max} - 1]$. Figure 5 represents the flowchart of the entire DB FBE algorithm.

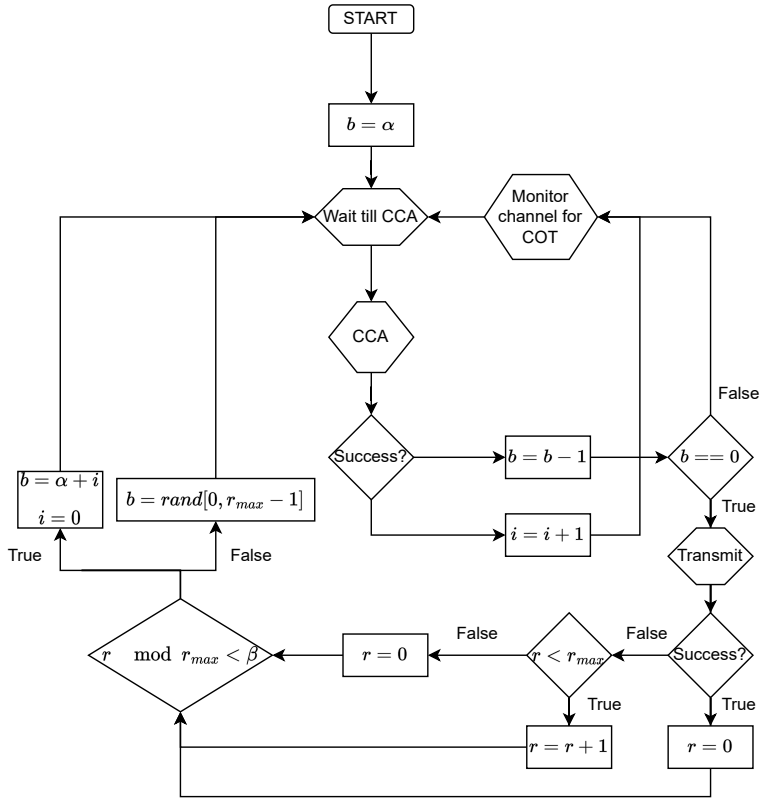

Figure 5. Flowchart of the DB FBE algorithm.

3.2.5. Enhanced FBE

Wijesiri and Li [35,39] define a method to improve fairness in channel access for LTE unlicensed (LTE-U) networks coexisting with Wi-Fi. Since LTE-U channel access shares some common features with FBE (most notably a duty cycle approach), we adapt this scheme and assess its performance in the following, referring to it as enhanced FBE (E-FBE). E-FBE introduces a backoff mechanism before channel access and defines two types of CCA: initial CCA (ICCA) and extended CCA (ECCA). ECCA is responsible for decrementing backoff after detecting an idle channel. On the other hand, during ICCA, backoff cannot be decremented even if this operation is successful. If an E-FBE node wants to access the channel, it will perform ICCA. If ICCA is successful, the node selects a random number N from the range $[0, Q]$, where Q defines the maximum backoff value. Then, the node enters the backoff phase, which starts with repeated ECCAs performed until $N = 0$. If a transmission occurs during ECCA or ICCA, the node has to become silent for the COT, wait for ICCA at the end of the FFP, and perform a new backoff value selection. When the node reaches $N = 0$, it immediately starts transmission. In Figure 6, an example of the backoff in E-FBE can be found. At the beginning, the node successfully completes ICCA and the first ECCA. During the second ECCA the channel is sensed as busy and the node is silent until the end of the FFP. Finally, the whole backoff phase is successfully performed and the channel is accessed.

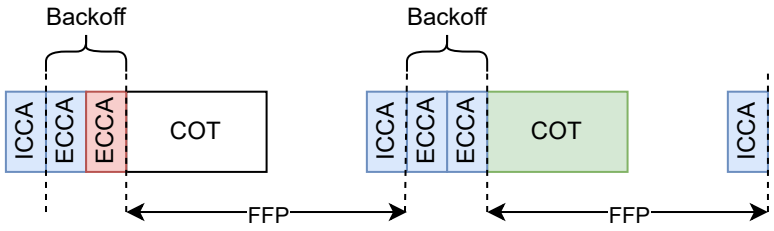

Figure 6. Operation of enhanced FBE.

3.2.6. Greedy-Enhanced FBE

Hu et al. [36] propose another approach for LTE-U which is similar to E-FBE. We refer to it as greedy-enhanced FBE (GE FBE). Contrary to E-FBE, ICCA is repeated until the node detects an idle channel, and if a transmission occurs during ECCA, ICCA is performed again, without a new backoff value selection. Figure 7 shows an example of the GE FBE procedure. Initially, the node chooses $N = 3$. ICCA is followed by a successful ECCA, but during the second ECCA, a transmission occurs. Then, ICCA is repeated twice until idle channel detection. Finally, the node performs the remaining ECCA successfully and begins transmission.

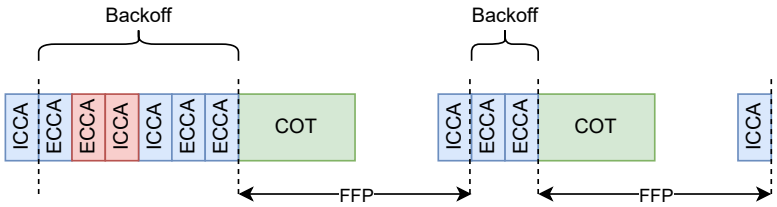

Figure 7. Operation of greedy-enhanced FBE.

3.2.7. BITR FBE

Wijesiri and Li [35] also design backoff and idle time reduction FBE (BITR FBE), an improvement to E-FBE. In BITR FBE, if backoff is interrupted, then the node's silence time is reduced to COT only. On the other hand, when the backoff countdown is successful, then the node follows the standard FFP. This behavior should equalize channel access opportunities and reduce the problem of single-node domination. An example of BITR FBE operation is presented in Figure 8.

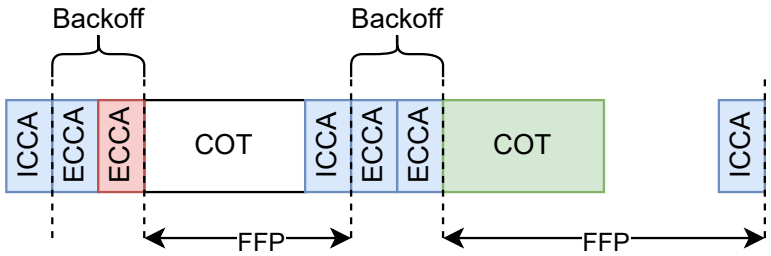

Figure 8. Operation of BITR FBE.

4. Simulation Model

In this section, we first describe our model assumptions and then the simulator used to evaluate the performance of the various FBE variants. Next, we introduce the metrics used to assess performance. Finally, we perform several validation experiments to ensure that the simulator operates correctly.

4.1. Assumptions

For the network setting, we consider a smart grid deployment of FBE nodes, i.e., a fully controlled industrial network operating in a greenfield environment. An example of this generic setting is a smart grid neighborhood area network [40] operating on a dedicated frequency. We are interested in determining the upper-bound performance of FBE and its variants. Therefore, we focus on network saturation conditions (i.e., a full-buffer model), although our implementation also supports a constant-rate traffic generator. Furthermore, since we assess channel access performance, we assume perfect channel conditions and no hidden nodes. Finally, we limit the study to downlink communication only and assume that acknowledgments are sent out of band (which is reasonable for NR-U operation).

4.2. Simulator

Discrete-event simulators are an appropriate tool for evaluating channel access mechanisms. In contrast to analytical models, e.g., Markov chains, these simulators allow each contending node to be treated independently. As we later show, with this approach we can easily identify improper channel access behavior, e.g., domination by a single node (Figure 9). Furthermore, we can rapidly conduct a performance analysis, evaluating upper bounds, as well as a coexistence analysis between competing FBE variants.

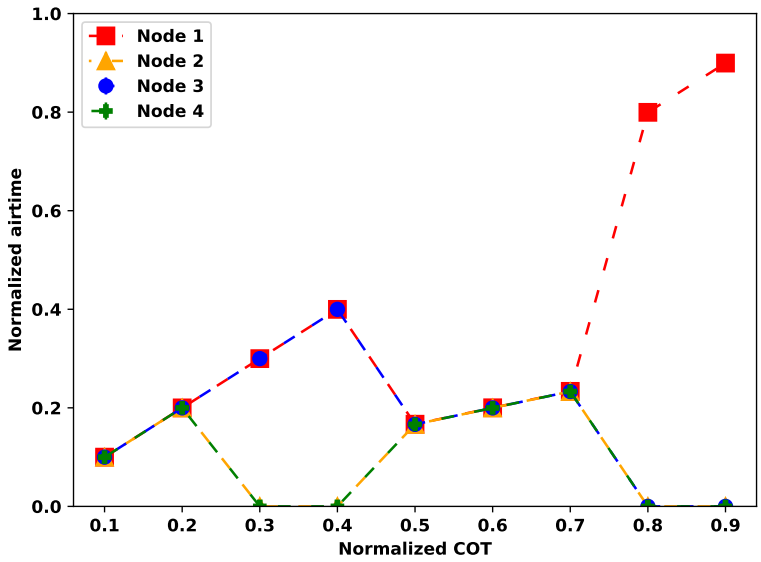

Figure 9. Validation of standard FBE. COT is normalized with respect to FFP.

To the best of our knowledge, there are no open-source network simulators available that implement FBE channel access or any of its variants. Therefore, we contribute our open-source simulator (https://github.com/marcink2138/NRUSharp, accessed on 24 December 2023), implemented in SimSharp (https://github.com/heal-research/SimSharp, accessed on 24 December 2023), with a .NET port of SimPy—a Python-based discrete-event simulation framework. Our simulator acts as an easily extensible library, which allows users to create their own test scenarios by creating simple C# scripts, with the .NET framework in version 7.0 or higher. The simulator is designed to be free of hard-coded variables, which means that the user can configure the node parameters. Furthermore, we design a set of utility classes which expedites the process of scenario configuration. We follow the operation principles of the NR-U SimPy simulator (https://github.com/marekzajac97/nru-channel-access, accessed on 24 December 2023), a discrete-event simulator successfully used in studies of NR-U operating in LBE mode [41,42].

In terms of implementation, our code works as follows. Each variant of FBE is represented by its own class that extends `AbstractFbeNode`. The `AbstractFbeNode` class contains basic definitions of methods defined in the `INode` interface and holds common properties, e.g., the objects responsible for storing node simulation results, while the FBE variant classes are focused on implementing the particular algorithms described in Section 3.2. Each node stores the same references to the `IChannel` interface and the `Simulation` class, which is responsible for holding queues, scheduling, and processing events generated by nodes. In our case, the `IChannel` interface is implemented by the `Channel` class, which holds a list of objects performing CCA (`ccaList`) and a list of each node with ongoing transmissions (`transmissionList`) along with the current timestamp. If the FBE node wants to sense the channel, then it has to append a reference to itself to `ccaList` and leave this list, regardless of status, at the end of CCA. During transmission, this node notifies all nodes in `ccaList` and `transmissionList` by interrupting their current simulation processes. An interruption of the transmission process is treated as a collision, whereas an interruption

of the CCA process denotes the detection of an ongoing transmission. Furthermore, each simulation scenario can be described by the `SimulationDescription` class, which stores information about the retransmission counter, simulation time, and simulation matrix. The simulation matrix holds information about simulation runs and references to configured nodes in a particular simulation run. The simulator also supports various logging verbosity levels to help users during validation and debugging.

4.3. Metrics

The simulator calculates several metrics to evaluate performance. Each node collects the following information:

- number of successful and failed transmissions;
- airtime—the time spent on successful transmissions;
- channel access delay—the time elapsed between the start of two consecutive successful transmissions.

These per-node metrics are merged after each simulation to calculate the following overall network performance metrics:

- normalized airtime—ratio of all nodes' aggregated airtime to the simulation time (this channel efficiency measure is an equivalent of throughput);
- Jain's fairness index—calculated based on per-node airtime to describe how well the channel (as a resource) is shared between nodes. It takes values from the range $\left[\frac{1}{n}, 1\right]$, where n indicates the number of nodes and 1 indicates perfect fairness.

4.4. Validation

Since there are no existing simulation tools that implement FBE channel access, we validate our implementation by describing the results of an explainable (test) scenario. The scenario is performed for each of the FBE variants, with the common simulation parameters listed in Table 1. We achieve perfect node coordination by configuring evenly spread shifts, i.e., 0 ms, 2.5 ms, 5 ms, and 7.5 ms for the four nodes, respectively. Note that this scenario is for validation only, while a full performance analysis is provided in the subsequent section. Specifically, we provide per-node results and derive conclusions based on observed behavior through a study of the presented metrics and an in-depth analysis of the logs. The error bars in the figures represent the 95% confidence intervals, although they are not always visible because there is little or no randomness in many variants of FBE.

Table 1. Simulation parameter settings.

Parameter	Value
No. of nodes	4
FFP	10 ms
COT	From 1 ms to 9 ms
Simulation time	20 s
Independent runs	10

For standard FBE, Figure 9 represents a plot of normalized airtime as a function of normalized COT (ratio of COT to FFP). As depicted, for particular values of normalized COT, some nodes greedily access the channel. Due to the periodicity of FFP and the assumption that the network is constantly saturated, it is easy to provide a formula predicting the order of transmitting nodes:

$$N_{seq} = (C_{seq} + Z) \mod M + 1, \tag{2}$$

where N_{seq} is the sequence number of the node which performs the next transmission, C_{seq} is the sequence number of the currently transmitting node, Z identifies the number of CCAs interrupted by the currently transmitting node, and M is the overall number of participating nodes (here, $M = 4$). For the lowest values of COT, the channel is fairly shared

between nodes, due to perfect node coordination, in which transmissions do not overlap with CCA periods, the parameter Z is equal to zero, and a round-robin scheme is followed. For further values of normalized COT, between 0.3 and 0.4, the channel becomes dominated by the first and third nodes: their transmissions constantly interrupt the CCAs of the second and fourth nodes, and in accordance with (2) the following pattern is achieved:

$$N_1 \rightarrow N_3 \rightarrow N_1 \rightarrow N_3.$$

When COT $\in [0.5, 0.7]$ the CCA operation of two consecutive nodes is interrupted and $Z = 2$, resulting in the following transmission pattern:

$$N_1 \rightarrow N_4 \rightarrow N_3 \rightarrow N_2.$$

For higher COT values, the node with the lowest offset continuously interrupts the CCA procedures of other participants ($Z = 3$) and accesses the channel. Hence, careful configuration is required before deploying standard FBE in a production environment, to reduce the risk of node domination.

The simulator also introduces a constant-rate traffic generator, modeled with an exponential distribution. Each frame created by the traffic generator is described by its duration, expressed in microseconds, which identifies the airtime needed for a complete frame transmission. Furthermore, each node participating in the simulation has its own buffer. The implementation of the traffic generator is validated by a particular edge case in Figure 9 for a value of normalized COT equal to 0.4. The buffer size for each node is constant and set to 200 frames, while the value of lambda (mean frame arrival per millisecond) is successively doubled. The results of this scenario are depicted in Figure 10. For the lowest lambda values, the gaps between frame arrivals are large enough to guarantee an equal share of the channel. After exceeding a value of 1.28 frames/ms, network operation collapses (i.e., nodes have unequal channel access probabilities) and finally, under saturation, the channel becomes dominated by the first and third nodes. This behavior matches the results of Figure 9 for a normalized COT of 0.4, which implies the proper operation of the simulator also under non-saturation.

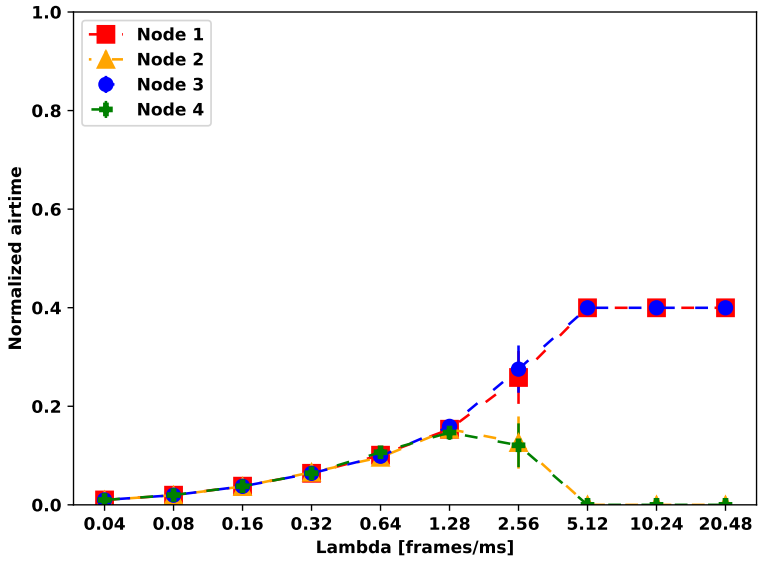

Figure 10. Results of standard FBE validation for a normalized COT of 0.4 with the use of a constant-rate traffic generator. Increasing lambda successfully reduces the transmission opportunities of the dominated nodes (cf. Figure 9). Note the log2 scale on the x-axis.

We now validate the implementation of the FBE variants. Figure 11a,b present results for fixed-muting FBE and random-muting FBE, respectively. In this case, the fixed-muting

FBE parameter N (number of muted periods after successful transmission) is equal to one, while for random muting the maximum number of continuous transmissions and muted periods are both set to five. Introducing these muted periods after a successful transmission reduces the node-domination problem, giving the opportunity to access the channel for nodes that under standard FBE would not be able to access the channel. However, for small normalized COT values (between 0.1 and 0.2), slightly worse performance can be observed than for standard FBE. For these low COT values, nodes achieve perfect coordination; there is no chance to interrupt a CCA procedure by other node transmissions, and introducing additional muted periods reduces the overall number of transmission opportunities.

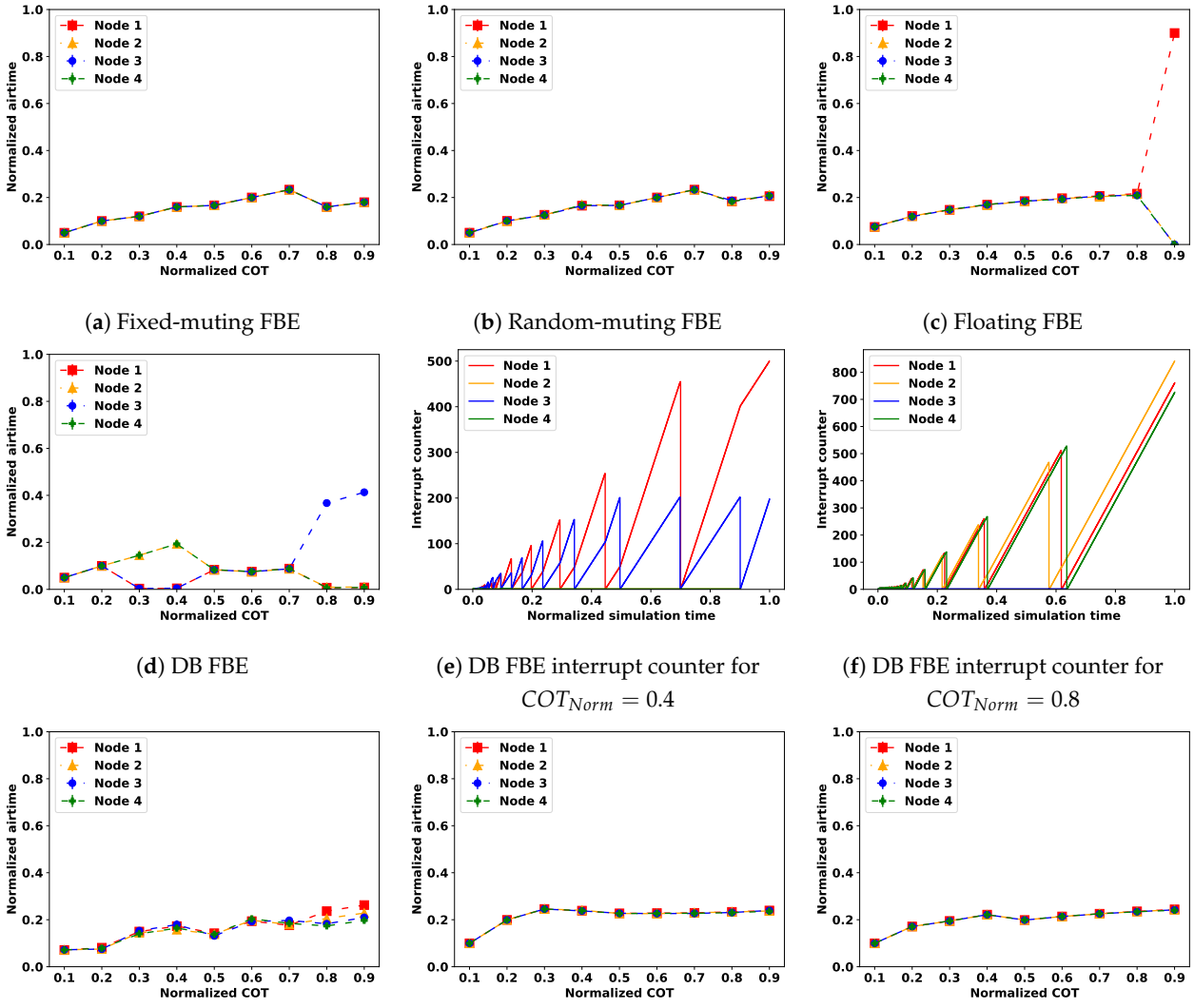

(**a**) Fixed-muting FBE (**b**) Random-muting FBE (**c**) Floating FBE

(**d**) DB FBE (**e**) DB FBE interrupt counter for $COT_{Norm} = 0.4$ (**f**) DB FBE interrupt counter for $COT_{Norm} = 0.8$

(**g**) Enhanced FBE (**h**) Greedy-enhanced FBE (**i**) BITR FBE

Figure 11. Validation of FBE variants.

Next, the validation results for floating FBE are depicted in Figure 11c. The curve of normalized airtime is similar for every node, regardless of offset, until an upper-bound condition is met. After exceeding this boundary COT value, the channel is completely dominated by the node with the lowest offset (here, the fourth node). This situation can occur only when the difference between the maximum offset of the fourth node's CCA inside its FFP ($CCA_{Offset,4}$) and the minimal transmission start time for the first node ($T_{Start,1}$) is less than the length of the COT (COT_1):

$$CCA_{Offset,4} - T_{Start,1} \leq COT_1. \quad (3)$$

The minimal transmission start, in the case of floating FBE, occurs when the node selects zero offset slots, and the CCA procedure occurs immediately after the start of the FFP. For the fourth node, CCA_{Offset} is the sum of the shift and the maximum number of selected slots multiplied by the length of the observation slot:

$$Shift_4 + \left\lfloor \frac{FFP_4 - COT_4 - CCA_4}{O_s} \right\rfloor \times O_s - CCA_4 \leq COT_1 \quad (4)$$

where $Shift_4$ — fourth node shift;
FFP_4 — fourth node FFP length;
COT_4 — fourth node COT length;
COT_1 — first node COT length.

Solving for COT_1 as an integer and for the known parameters of the fourth node in the last scenario, we obtain

$$COT_1 \geq 8741 \text{ µs}. \quad (5)$$

In floating FBE, this inequality is achieved for a normalized COT of 0.9, which results in the domination of the first node. We conclude that the improvement introduced in floating FBE does not always guarantee an equal share of the channel, and, similarly to standard FBE, careful configuration is required.

For DB FBE, the validation results are presented in Figure 11d. Similarly to standard FBE, DB FBE also suffers from node-domination problems. Moreover, according to the DB FBE backoff selection algorithm, the backoff value cannot be randomly selected. Nodes always know about ongoing transmissions: collisions are impossible, the retransmission counter is not incremented, and the threshold value β is never exceeded. For the lowest values of COT, as long as only one node wants to transmit a frame at a given time, a round-robin schedule is guaranteed. When the normalized COT is between 0.3 and 0.4, the channel is dominated by the second and fourth nodes, which continuously interrupt the channel monitoring phases, resulting in extremely high values of the interrupt counter (Figure 11e). Subsequently, transmissions interrupt the CCAs of two consecutive nodes, which again leads to a round-robin scheme. Finally, the channel is dominated by the third node due to the high values of the interrupt counter (Figure 11f). This behavior implies that DB FBE nodes must operate in synchronous mode (no shifts). Subsequently, we conclude that DB FBE cannot easily coexist with other channel access methods.

The results for enhanced FBE, greedy-enhanced FBE, and BITR FBE are shown in Figure 11g–i, respectively. As described in Section 3.2, these variants refrain from fully periodic transmissions by using a backoff mechanism. Therefore, every time one of the nodes dominates the channel, other nodes try to match the starts of their COTs with the dominant one. We illustrate this in the following way. Consider the case of enhanced FBE for a normalized COT of 0.9. When the first node successfully performs backoff, it gains channel access, transmits (when other nodes are checking for ongoing transmissions during ICCA), and then mutes itself for FFP minus CCA. The backoff mechanism in the first node constantly moves its COT forward in time until the other node's ICCA is not interrupted, and its own backoff procedure can be performed. Conversely, greedy-enhanced FBE does not select a new backoff value after unsuccessful ICCA or ECCA, but continuously samples the status of ongoing transmissions and can immediately access the channel, after deducting its own backoff, during the idle period of a previously transmitting node. Meanwhile, the introduction of the idle time reduction in BITR FBE accelerates the COT convergence process. Thus, both greedy-enhanced and BITR FBE achieve better performance, especially for larger COT values. We conclude that introducing backoff in enhanced, greedy-enhanced, and BITR FBE reduces the problem of node domination. Nevertheless, due to the increased probability of collisions, worse performance should be expected than in the case of variants that follow the FFP periodicity and are configured under perfect node coordination.

In summary, we have evaluated the performance of all available FBE variants in a specific scenario for varying COT durations. We are able to explain the behavior under all

cases and draw specific conclusions regarding further analysis (e.g., that DB FBE nodes must operate in synchronous mode). Thus, having validated our simulator, we proceed to study the upper-bound performance and coexistence capabilities of the FBE variants.

5. Performance Analysis

We conduct a performance analysis of FBE variants in two settings: (i) all nodes in the network use the same variant, and (ii) all nodes use different (competing) variants.

5.1. Homogeneous Networks

To evaluate overall performance in the homogeneous case, we measure the metrics defined previously as a function of an increasing number of nodes. We use two simulation approaches to depict crucial differences in the behavior of the variants. The first is the 'optimized parameter' approach. We select per-node parameters such that the performance of the whole network is similar, regardless of the number of contending nodes. To achieve this goal, we carefully tune the variant parameters (with a parameter sweep) to achieve the best performance for each case. These parameters include node shift (for perfect node coordination), FFP and COT durations, as well as variant-specific parameters. Examples of these parameters for standard FBE and fixed-muting FBE are given in Table 2. A complete listing, containing all variants, is provided in the online Supplementary Material (https://github.com/marcink2138/NRUSharp/blob/main/tests/README.MD, accessed on 24 December 2023). In the second, 'non-optimized parameter' approach, we use fixed parameter values for a varying number of contending nodes. The values are arbitrarily selected as those that optimize performance for eight competing nodes.

Table 2. Optimized simulation parameters for standard FBE and fixed-muting FBE for homogeneous networks.

Nodes	Standard FBE		Fixed-Muting FBE		
	FFP (µs)	COT (µs)	FFP (µs)	COT (µs)	*N*
2	1000	491	1000	491	0
4	2000	491	1000	491	1
8	4000	491	1000	491	3
16	8000	491	1000	491	7
32	10,000	303	1000	491	15

For the case of optimized parameters, the results are presented in Figure 12. We expect to see high fairness (indicative of good resource sharing) as well as low channel access delay and high channel efficiency (both indicative of a low number of collisions and 'silent' periods). We observe that all variants are able to achieve a constant and high value of fairness, close to one. The delay values increase with the number of competing nodes (which is expected) and are larger for the three random-backoff-based variants. There is more variance in the channel efficiency results. Although most variants can reach high values, four of them perform significantly worse. In the case of DB FBE, this is caused by the expensiveness of its backoff algorithm, whose convergence time grows with the number of nodes. For floating FBE it is impossible to achieve perfect node coordination due to its random offset before COT, while enhanced FBE suffers from collisions. Interestingly, the channel efficiency of random-muting FBE increases due to the existence of obligatory muted periods and their randomness. The best performance efficiency is achieved by standard FBE, as well as fixed-muting BITR and greedy-enhanced FBE. In particular, with a properly selected node shift, FFP, and COT length, it is possible to achieve a constant and almost perfect value of channel efficiency for standard and fixed-muting FBE. BITR FBE and greedy-enhanced FBE successfully reduce the number of possible collisions by either shortening the idle time after an unsuccessful backoff or constant channel sampling,

respectively. These features result in better channel utilization than in the case of the similar enhanced FBE using the same node shifts and maximal backoff counter values.

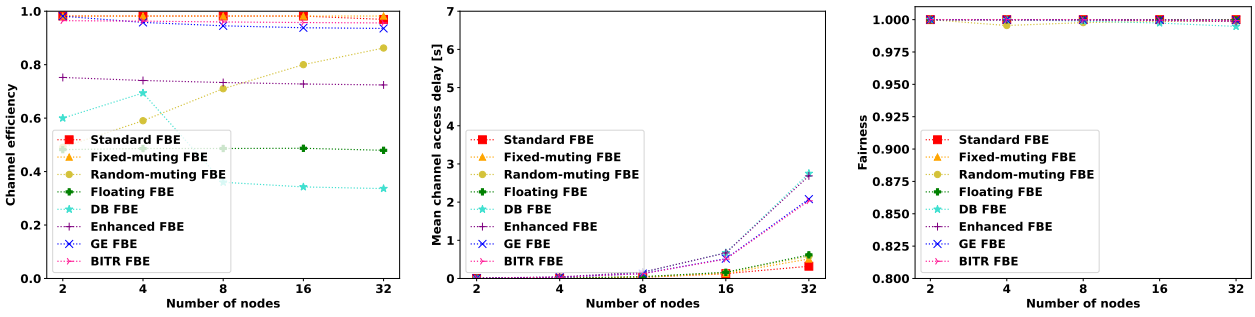

(**a**) Channel efficiency (**b**) Mean channel access delay (**c**) Fairness

Figure 12. Results for homogeneous networks under optimized parameters.

In Figure 13, we provide the simulation results for the non-optimized case. As expected, the measured metrics achieve the best values for eight nodes. However, changing the number of contending nodes without parameter optimization leads to significantly reduced performance. In the case of standard FBE, fixed-muting FBE, and random-muting FBE the main factor which determines this decrease is the periodicity of fixed frames. For non-optimized parameters, it is easy to cause overlapping of FFPs, which then leads to the synchronization issue depicted in Figure 2a and either constant collisions or, in the best case, only occasional transmissions. Floating FBE suffers from the problem of single-node domination, which is proven by unacceptable values of mean channel access delay and fairness, while also increasing channel efficiency. It turns out that DB FBE, greedy-enhanced FBE, and BITR FBE achieve similar results as in the optimized case, but with a visible decrease in channel efficiency and an increase in mean channel access delay. However, they maintain a high value of fairness. The worst performance among the backoff-based variants is achieved by enhanced FBE, where for 32 nodes, the value of mean channel access delay almost doubles.

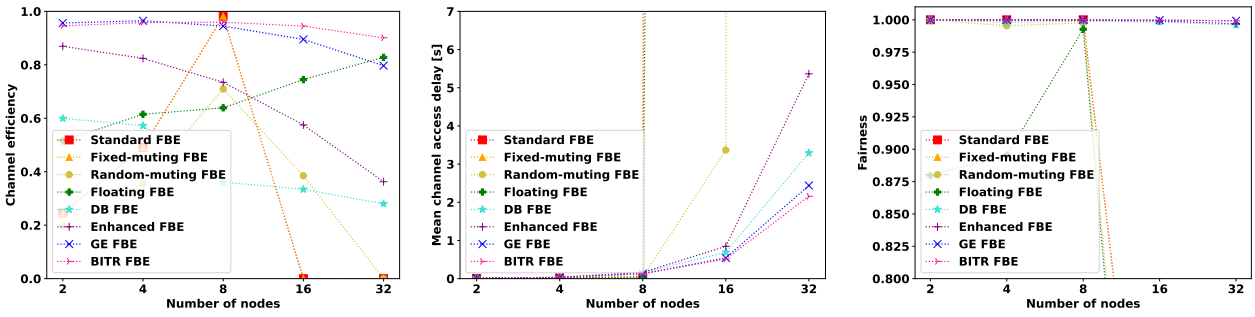

(**a**) Channel efficiency (**b**) Mean channel access delay (**c**) Fairness

Figure 13. Results for homogeneous networks under non-optimized parameters.

In summary, these results show that improper selection of FBE parameters can cause serious channel access problems. Any additional node is able to desynchronize all others and reduce overall performance. We conclude that for these variants, both parameter and *shift* optimization are required for each new node joining the channel access contention. Such optimization could be performed by an external controller, responsible for monitoring and reconfiguring nodes operating in the same channel.

5.2. Heterogeneous Networks

We now evaluate the coexistence performance of FBE variants by comparing two variants against each other. Each scenario involves eight nodes, half operating in a different variant. Similarly to the previous study, each network is optimally configured as if it were operating in an exclusive environment, and the evaluation is conducted based on the metrics of fairness and channel efficiency. To make the results more concise, we refrain from displaying the channel access delay. Although there are eight possible variants, which would lead to $\binom{8}{2} = 28$ independent comparisons, we reduce their number by not including the following:

- DB FBE vs. all other variants;
- Standard FBE vs. fixed-muting FBE;
- Standard FBE vs. random-muting FBE;
- Fixed-muting FBE vs. random-muting FBE.

Our justification for this omission is as follows. In DB FBE, the deterministic-backoff algorithm requires homogeneous networks, due to its expensiveness in convergence. Each of the seven other variants dominates DB FBE by performing transmissions during the channel monitoring phase. The interruption of this phase increases the value of the interrupt counter, which increases the DB FBE backoff. For standard, fixed-muting, and random-muting FBE, the conclusions are also obvious. If the shift of participating nodes is the same or the CCAs overlap, constant collisions are expected. Achieving perfect node coordination through shift optimization leads to the best performance of standard FBE, while the results of fixed-muting and random-muting FBE are closely related to the values of M and N. Thus, we can expect either lower performance of fixed-muting and random-muting FBE or the dominance of standard FBE nodes.

Figure 14 shows the results of the remaining 18 test cases of heterogeneous networks. We expect the aggregate normalized airtime of each variant to be close to 0.5, while the channel efficiency and fairness should be close to 1. We first look at the coexistence results of standard FBE (Figure 14a–c,j). The parameter setup for standard FBE is again focused on achieving the highest possible channel efficiency. This configuration results in complete channel dominance by standard FBE in each of the tests performed. The main reason behind such behavior is connected with perfect node coordination: the difference between two consecutive transmissions for standard FBE nodes is 9 µs—it becomes almost impossible for contending variants to decrement their backoff (if supported by that variant) and transmit in such short time windows.

Similarly to results from previous subsections, the muted periods introduced by fixed-muting and random-muting FBE give an opportunity for other variants to successfully perform transmissions. However, in almost all cases, the performance of fixed-muting and random-muting FBE is better than that of other variants (e.g., Figure 14d,i). The only exception is greedy-enhanced FBE (Figure 14e,h). Its aggressive, constant sampling gives the opportunity to grab the channel faster than other coexisting variants. In the case of floating FBE, each node starts at the same time, due to the unwanted risk of single-node domination, as presented in Section 4.4. Setting the shift of floating FBE nodes to the same value guarantees that potential transmissions depend only on the selected offset. Unfortunately, selecting the high offset by floating FBE nodes (which frequently occurs in the case of common FFP and COT parameters) gives other variants time to access the channel, which results in the lower performance of floating FBE. In the case of enhanced and BITR FBE, the worst results are achieved by enhanced FBE. An enhanced FBE node has to wait a whole FFP before the next backoff, which for the low COT to FFP ratio gives much time for other variants. In contrast, BITR FBE with its idle time reduction after unsuccessful backoff improves overall performance and achieves good coexistence with fixed-muting and random-muting FBE.

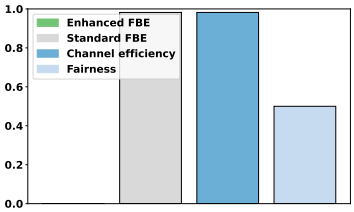

(**a**) Standard FBE vs. Enhanced FBE

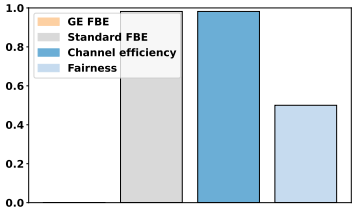

(**b**) Standard FBE vs. GE FBE

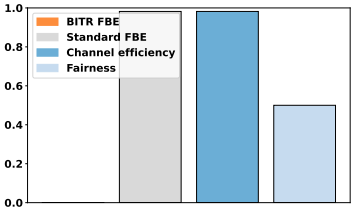

(**c**) Standard FBE vs. BITR FBE

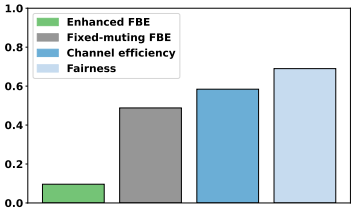

(**d**) Fixed-Muting FBE vs. Enhanced FBE

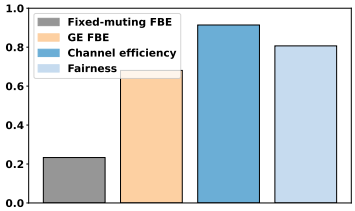

(**e**) Fixed-Muting FBE vs. GE FBE

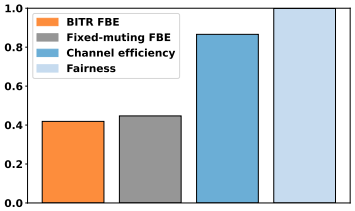

(**f**) Fixed-Muting FBE vs. BITR FBE

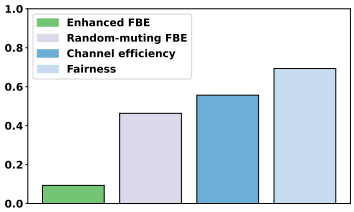

(**g**) Random-Muting FBE vs. Enhanced FBE

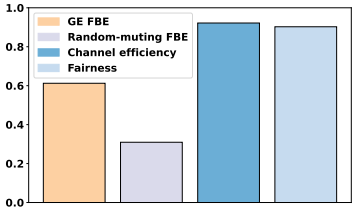

(**h**) Random-Muting FBE vs. GE FBE

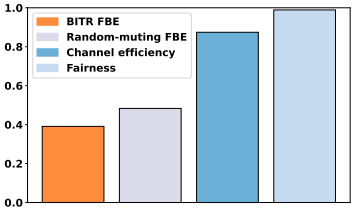

(**i**) Random-Muting FBE vs. BITR FBE

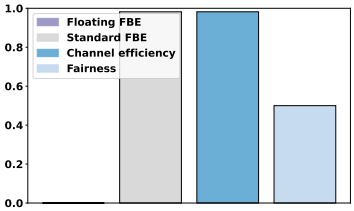

(**j**) Floating FBE vs. Standard FBE

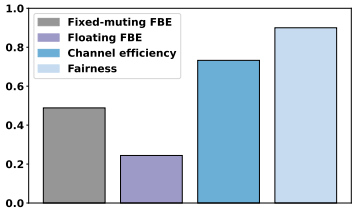

(**k**) Floating FBE vs. Fixed-Muting FBE

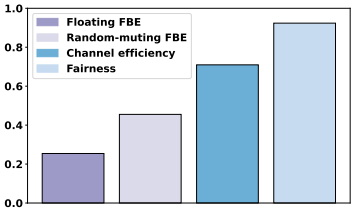

(**l**) Floating FBE vs. Random-Muting FBE

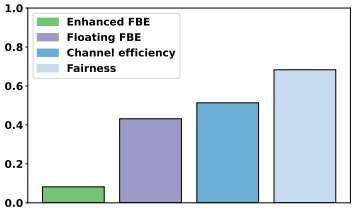

(**m**) Enhanced FBE vs. Floating FBE

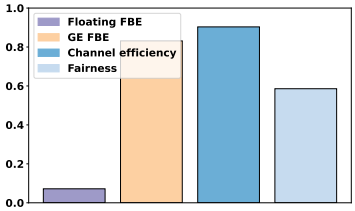

(**n**) Floating FBE vs. GE FBE

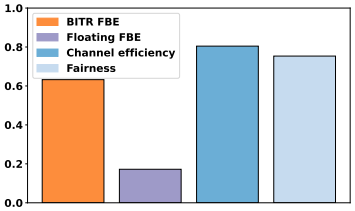

(**o**) Floating FBE vs. BITR FBE

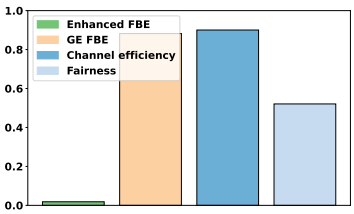

(**p**) Enhanced FBE vs. GE FBE

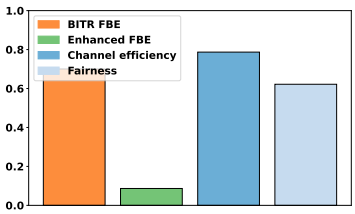

(**q**) Enhanced FBE vs. BITR FBE

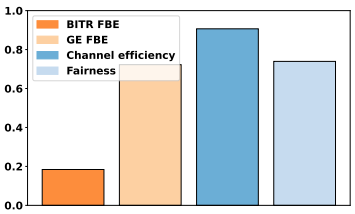

(**r**) GE FBE vs. BITR FBE

Figure 14. Results for heterogeneous networks: eight nodes in total, half operating under one variant. Each plot contains the aggregate normalized airtime of each variant (first two bars), the overall channel efficiency, and fairness.

The coexistence results are summarized in Table 3. In this study, fairness is the most important metric. The highest fairness is achieved by random-muting FBE. Fortunately, it exhibits quite good efficiency. Meanwhile, low fairness with near-perfect channel efficiency is meaningless, as indicated by standard FBE's results. Greedy-enhanced FBE has the second highest efficiency, but is aggressive in acquiring channel resources. Thus, we conclude that there is still room for improvement in designing an FBE variant with good coexistence qualities.

Table 3. Summary of coexistence performance in the studied heterogeneous networks. The channel efficiency refers to the overall airtime observed in scenarios which had the competing variant, while the variant airtime refers only to the airtime used by the given variant.

Variant	Mean Channel Efficiency	Mean Fairness	Mean Variant Airtime
Standard FBE	0.98	0.5	0.98
Fixed-Muting FBE	0.77	0.85	0.41
Random-Muting FBE	0.76	0.88	0.42
Floating FBE	0.77	0.72	0.20
Enhanced FBE	0.72	0.61	0.06
Greedy-Enhanced FBE	0.92	0.67	0.62
BITR FBE	0.87	0.76	0.38

6. Conclusions

In this paper, we have analyzed the performance of FBE channel access mechanisms and provided the following contributions. First, we have implemented, validated, and released a fully functional open-source discrete-event simulator which can be used to study the performance of FBE and its variants. Second, with this simulator, we performed a detailed investigation of FBE homogeneous networks with optimized and non-optimized node parameters as well as an analysis of the coexistence of FBE variants. Third, based on our research results, the following general conclusions can be drawn:

- Variants which follow a strict periodicity of fixed frame periods (standard FBE, fixed-muting FBE, random-muting FBE) cannot operate with synchronized COTs, because this leads to low channel access probabilities, and in the extreme case (saturated network) to a lack of successful transmissions. In such a situation, synchronized nodes attempt to transmit at the same time, and the problem of constant collisions occurs. Of all the variants studied, only our adaptation of deterministic-backoff in FBE requires such synchronization. Otherwise, DB FBE is not able to fully perform and force contending nodes to follow the expected round-robin scheme.
- Deployment of FBE networks with standard FBE, fixed-muting FBE, random-muting FBE, and floating FBE variants requires a detailed analysis of proper parameter selection to eliminate potential issues with a node or group of nodes that completely dominate access to channel resources.
- Observing the design of floating FBE, it seems to be a variant that comes with an out-of-the-box solution for single-node domination. However, we observe that there are some edge cases in which a single floating FBE node can dominate the channel. Moreover, the random offset inside floating FBE's FFP hinders proper synchronization with an NR-U slot boundary.
- Comparing results for homogeneous networks with optimized and non-optimized parameters, we conclude that FBE networks require some kind of external controller responsible for selecting and updating parameters for each node newly attached to the wireless network. It was shown that, in the optimized parameter case, all presented FBE variants perform well and achieve consistently high fairness. In the non-optimized scenario, each new node increases the possibility of network desynchronization, which leads to a complete waste of channel resources. The BITR FBE and greedy-enhanced FBE variants seem to be the most resistant to uncontrolled environments.

- In coexistence scenarios, standard FBE with perfect node coordination and under optimal parameters can completely dominate other variants. The feature of muted periods added in fixed-muting and random-muting FBE increases the transmission opportunities of other variants. In general, the following pairs of variants exhibit good coexistence: fixed-muting with random-muting FBE and BITR with floating FBE.
- In the case of variants that introduce backoff, the lack of handicap after unsuccessful CCA in enhanced FBE results in the lowest performance, while idle time reduction in BITR FBE improves its fairness and coexistence abilities. In direct comparisons between these variants, GE FBE takes the most channel resources due to its aggressive channel sampling. Such greedy behavior requires constantly turning on the receivers until completing the backoff, which might result in higher energy consumption.
- Similarly to floating FBE, it is difficult to match the start of COT with a synchronization slot boundary in all backoff-based variants.

In summary, as future work, we foresee addressing the problem of the selection of efficient general and variant-specific FBE parameters, especially in dynamic scenarios. Another interesting research topic is the coexistence with networks using LBE-based channel access (including Wi-Fi). Finally, our implementation can be extended by an additional controller module, which seems to be an inevitable element of such networks [27].

Supplementary Materials: The following supporting information can be downloaded at: https://github.com/marcink2138/NRUSharp/blob/main/tests/README.MD, accessed on 24 December 2023.

Author Contributions: Conceptualization, M.K. and S.S.; methodology, M.K. and S.S.; writing—original draft preparation, M.K.; writing—review and editing, S.S.; visualization, M.K.; project administration, S.S.; funding acquisition, S.S. All authors have read and agreed to the published version of the manuscript.

Funding: This research received no external funding.

Data Availability Statement: The data presented in this study are available online at: https://github.com/marcink2138/NRUSharp/tree/main/data, accessed on 24 December 2023.

Conflicts of Interest: The authors declare no conflict of interest.

References

1. Suhaimy, N.; Radzi, N.A.M.; Ahmad, W.S.H.M.W.; Azmi, K.H.M.; Hannan, M.A. Current and future communication solutions for smart grids: A review. *IEEE Access* **2022**, *10*, 43639–43668. [CrossRef]
2. Sharma, D.K.; Rapaka, G.K.; Pasupulla, A.P.; Jaiswal, S.; Abadar, K.; Kaur, H. A review on smart grid telecommunication system. *Mater. Today Proc.* **2022**, *51*, 470–474. [CrossRef]
3. Gupta, M.; Kumar, V. A survey on spectrum sharing techniques in cognitive radio-based smart grids. In *3rd International Conference on Wireless, Intelligent and Distributed Environment for Communication: WIDECOM 2020*; Springer: Berlin/Heidelberg, Germany, 2020; pp. 113–122. [CrossRef]
4. Mekonnen, Y.; Haque, M.; Parvez, I.; Moghadasi, A.; Sarwat, A. LTE and Wi-Fi coexistence in unlicensed spectrum with application to smart grid: A review. In Proceedings of the 2018 IEEE/PES Transmission and Distribution Conference and Exposition (T & D), Denver, CO, USA, 16–19 April 2018; IEEE: Piscataway, NJ, USA, 2018; pp. 1–5. [CrossRef]
5. Naik, G.; Park, J.M.; Ashdown, J.; Lehr, W. Next generation Wi-Fi and 5G NR-U in the 6 GHz bands: Opportunities and challenges. *IEEE Access* **2020**, *8*, 153027–153056. [CrossRef]
6. Broadband Radio Access Networks (BRAN). *5 GHz RLAN; Harmonised Standard Covering the Essential Requirements of Article 3.2 of Directive 2014/53/EU*; Technical Report EN 301 893; ETSI: Sophia Antipolis, France, 2017.
7. Parvez, I.; Sarwat, A. A Spectrum Sharing based Metering Infrastructure for Smart Grid Utilizing LTE and WiFi. *Adv. Sci. Technol. Eng. Syst. J.* **2019**, *4*, 70–77. [CrossRef]
8. Song, H.; Cui, Q.; Gu, Y.; Stüber, G.L.; Li, Y.; Fei, Z.; Guo, C. Cooperative LBT design and effective capacity analysis for 5G NR ultra dense networks in unlicensed spectrum. *IEEE Access* **2019**, *7*, 50265–50279. [CrossRef]
9. Daraseliya, A.; Korshykov, M.; Sopin, E.; Moltchanov, D.; Andreev, S.; Samouylov, K. Coexistence analysis of 5G NR unlicensed and WiGig in millimeter-wave spectrum. *IEEE Trans. Veh. Technol.* **2021**, *70*, 11721–11735. [CrossRef]
10. Loginov, V.; Khorov, E.; Lyakhov, A.; Akyildiz, I.F. CR-LBT: Listen-before-talk with collision resolution for 5G NR-U networks. *IEEE Trans. Mob. Comput.* **2021**, *21*, 3138–3149. [CrossRef]

11. Kosek-Szott, K.; Valvo, A.L.; Szott, S.; Gallo, P.; Tinnirello, I. Downlink channel access performance of NR-U: Impact of numerology and mini-slots on coexistence with Wi-Fi in the 5 GHz band. *Comput. Netw.* **2021**, *195*, 108188. [CrossRef]
12. Tinnirello, I.; Lo Valvo, A.; Szott, S.; Kosek-Szott, K. No reservations required: Achieving fairness between Wi-Fi and NR-U with self-deferral only. In Proceedings of the 24th International ACM Conference on Modeling, Analysis and Simulation of Wireless and Mobile Systems, Alicante, Spain, 22–26 November 2021; pp. 115–124. [CrossRef]
13. Ma, Y.; Mosleh, S.; Coder, J. Analyzing 5G NR-U and WiGig coexistence with multiple-beam directional LBT. In Proceedings of the 2022 IEEE 19th Annual Consumer Communications & Networking Conference (CCNC), Las Vegas, NV, USA, 8–11 January 2022; IEEE: Piscataway, NJ, USA, 2022; pp. 272–275. [CrossRef]
14. Pei, X.; Qian, H.; Wang, H.; Kang, K. An Improved Listen-Before-Talk Scheme for Uplink Multiple Access in 5G Unlicensed Band. *IEEE Internet Things J.* **2022**, *9*, 19843–19853. [CrossRef]
15. Ren, Q.; Wang, B.; Zheng, J.; Zhang, Y. Performance Modeling of an NR-U and WiFi Coexistence System Using the NR-U Category-4 LBT Procedure and WiFi DCF Mechanism in the Presence of Hidden Nodes. *IEEE Trans. Veh. Technol.* **2023**, *72*, 14801–14814. [CrossRef]
16. Wszołek, J.; Ludyga, S.; Anzel, W.; Szott, S. Revisiting LTE LAA: Channel Access, QoS, and Coexistence with WiFi. *IEEE Commun. Mag.* **2021**, *59*, 91–97. [CrossRef]
17. Bajracharya, R.; Shrestha, R.; Jung, H. Bandit Approach for Fair and Efficient Coexistence of NR-U in Unlicensed Bands. *IEEE Trans. Veh. Technol.* **2022**, *72*, 5208–5223. [CrossRef]
18. Bajracharya, R.; Shrestha, R.; Jung, H. Future is unlicensed: Private 5G unlicensed network for connecting industries of future. *Sensors* **2020**, *20*, 2774. [CrossRef] [PubMed]
19. Kini, A.V.; Canonne-Velasquez, L.; Hosseinian, M.; Rudolf, M.; Stern-Berkowitz, J. Wi-Fi-LAA coexistence: Design and evaluation of Listen Before Talk for LAA. In Proceedings of the 2016 Annual Conference on Information Science and Systems (CISS), Princeton, NJ, USA, 16–18 March 2016; pp. 157–162. [CrossRef]
20. Khairy, S.; Cai, L.X.; Cheng, Y.; Han, Z.; Shan, H. A Hybrid-LBT MAC with Adaptive Sleep for LTE LAA Coexisting with Wi-Fi over Unlicensed Band. In Proceedings of the GLOBECOM 2017—2017 IEEE Global Communications Conference, Singapore, 4–8 December 2017; pp. 1–6. [CrossRef]
21. Huynh, C.K.; Yun, D.W.; Choi, J.P.; Lee, W.C. Performance analysis for coexistence of LTE-LAA and Wi-Fi systems in the spatial, time, spectrum domain. *ICT Express* **2019**, *5*, 72–76. [CrossRef]
22. Kiran, V.; Telkar, P.S.; Nayak, D.; Raj, D.R. Wi-Fi and LTE Coexistence in Unlicensed Spectrum. In *IOT with Smart Systems: Proceedings of ICTIS 2021*; Springer: Berlin/Heidelberg, Germany, 2022; Volume 2, pp. 773–783.
23. Li, Y.; Zheng, J.; Li, Q. Enhanced listen-before-talk scheme for frequency reuse of licensed-assisted access using LTE. In Proceedings of the 2015 IEEE 26th Annual International Symposium on Personal, Indoor, and Mobile Radio Communications (PIMRC), Hong Kong, China, 30 August–2 September 2015; pp. 1918–1923. [CrossRef]
24. Sutton, G.J.; Liu, R.P.; Guo, Y.J. Coexistence performance and limits of frame-based listen-before-talk. *IEEE Trans. Mob. Comput.* **2019**, *19*, 1084–1095. [CrossRef]
25. Abdelfattah, A.; Malouch, N.; Ling, J. Analytical evaluation and potentials of frame based equipment for LTE-LAA/Wi-Fi coexistence. In Proceedings of the 2019 IEEE Symposium on Computers and Communications (ISCC), Barcelona, Spain, 29 June–3 July 2019; IEEE: Piscataway, NJ, USA, 2019; pp. 1–7. [CrossRef]
26. Park, S.; Ryu, H.; Kim, Y.; Han, J.K. Performance of Channel Access Mechanisms for 5G Industrial-IoT over Unlicensed Bands. In Proceedings of the 2021 IEEE 94th Vehicular Technology Conference (VTC2021-Fall), Norman, OK, USA, 27–30 September 2021; pp. 1–5. [CrossRef]
27. Maldonado, R.; Rosa, C.; Pedersen, K.I. A Fully Coordinated New Radio-Unlicensed System for Ultra-Reliable Low-Latency Applications. In Proceedings of the 2020 IEEE Wireless Communications and Networking Conference (WCNC), Seoul, Republic of Korea, 25–28 May 2020; IEEE: Piscataway, NJ, USA, 2020; pp. 1–6. [CrossRef]
28. Le, T.K.; Kaltenberger, F.; Salim, U. Dynamic switch between load based and frame based channel access mechanisms in unlicensed spectrum. In Proceedings of the 2021 IEEE Global Communications Conference (GLOBECOM), Madrid, Spain, 7–11 December 2021; IEEE: Piscataway, NJ, USA, 2021; pp. 1–6. [CrossRef]
29. Nobar, S.K.; Ahmed, M.H.; Morgan, Y.; Mahmoud, S. Joint channel assignment and occupancy time optimization in frame-based listen-before-talk. *IEEE Commun. Lett.* **2019**, *24*, 695–699. [CrossRef]
30. Wei, N.; Lin, X.; Xiong, Y.; Chen, Z.; Zhang, Z. Joint listening, probing, and transmission strategies for the frame-based equipment in unlicensed spectrum. *IEEE Trans. Veh. Technol.* **2017**, *67*, 1750–1764. [CrossRef]
31. Li, J.; Shan, H.; Huang, A.; Yuan, J.; Cai, L.X. Modelling of synchronisation and energy performance of FBE-and LBE-based standalone LTE-U networks. *J. Eng.* **2017**, *2017*, 292–299. [CrossRef]
32. Samsung. Channel Access Procedures for NR-U. Technical Report R1-1912449, 3rd Generation Partnership Project (3GPP). 2019. Available online: https://www.3gpp.org/ftp/TSG_RAN/WG1_RL1/TSGR1_99/Docs/R1-1912449.zip (accessed on 24 December 2023).
33. MediaTek Inc. Remaining Details in Channel Access Procedures. Technical Report R1-1912088, 3rd Generation Partnership Project (3GPP). 2019. Available online: https://www.3gpp.org/ftp/TSG_RAN/WG1_RL1/TSGR1_99/Docs/R1-1912088.zip (accessed on 24 December 2023).

34. ZTE and Sanechips. Remaining Issues on Channel Access Procedure for NR-U. Technical Report R1-1911822, 3rd Generation Partnership Project (3GPP). 2019. Available online: https://www.3gpp.org/ftp/TSG_RAN/WG1_RL1/TSGR1_99/Docs/R1-1911822.zip (accessed on 24 December 2023).
35. Wijesiri, G.P.; Li, F.Y. Frame based equipment medium access in LTE-U: Mechanism enhancements and DTMC modeling. In Proceedings of the GLOBECOM 2017—2017 IEEE Global Communications Conference, Singapore, 4–8 December 2017; IEEE: Piscataway, NJ, USA, 2017; pp. 1–6. [CrossRef]
36. Hu, H.; Zheng, M.; Yu, K.; Zhou, B. Enhanced listen-before-talk scheme for LTE in unlicensed band. In Proceedings of the 2016 6th International Conference on Electronics Information and Emergency Communication (ICEIEC), Beijing, China, 17–19 June 2016; IEEE: Piscataway, NJ, USA, 2016; pp. 168–173. [CrossRef]
37. Chen, H.Y.; Wang, S.S.; Sheu, S.T. Reliability improvement of frame-based equipment for ultra-reliable and low latency communication in unlicensed spectrum. *Int. J. Ad Hoc Ubiquitous Comput.* **2022**, *39*, 130–140. [CrossRef]
38. Kosek-Szott, K.; Szott, S.; Valvo, A.L.; Tinnirello, I. DB-LBT: Deterministic Backoff with Listen Before Talk for Wi-Fi/NR-U Coexistence in Shared Bands. In Proceedings of the MASCOTS 2022: 30th International Symposium on Modeling, Analysis, and Simulation of Computer and Telecommunication Systems, Nice, France, 18–20 October 2022; pp. 168–175. [CrossRef]
39. Wijesiri, G.P.; Li, F.Y. Enabling Backoff and Eliminating Redundant Idle Period for Medium Access in LTE-U. In Proceedings of the 2017 IEEE 86th Vehicular Technology Conference (VTC-Fall), Toronto, ON, Canada, 24–27 September 2017; pp. 1–5. [CrossRef]
40. Astudillo León, J.P.; Duenas Santos, C.L.; Mezher, A.M.; Cárdenas Barrera, J.; Meng, J.; Castillo Guerra, E. Exploring the potential, limitations, and future directions of wireless technologies in smart grid networks: A comparative analysis. *Comput. Netw.* **2023**, *235*, 109956. [CrossRef]
41. Zając, M.; Szott, S. Resolving 5G NR-U Contention for Gap-Based Channel Access in Shared Sub-7 GHz Bands. *IEEE Access* **2022**, *10*, 4031–4047. [CrossRef]
42. Akbar Basha, K.M.; Baswade, A.M. Numerology-Aware MCOT Selection for Improving Fairness in 5G NR-U Networks. *IEEE Commun. Lett.* **2023**, *27*, 1045–1049. [CrossRef]